

A Spatio-temporal CP decomposition analysis of New England region in the US

Fatoumata Sanogo^a

^aBates College Mathematics Department

ARTICLE INFO

Keywords:

Tensor
PCA
Clustering
CP Decomposition
Spatio temporal data

ABSTRACT

Spatio temporal data consist of measurement for one or more raster fields such as weather, traffic volume, crime rate, or disease incidents. Advances in modern technology have increased the number of available information for this type of data hence the rise of multidimensional data. In this paper we take advantage of the multidimensional structure of the data but also its temporal and spatial structure. In fact, we will be using the NCAR Climate Data Gateway website which provides data discovery and access services for global and regional climate model data. The daily values of total precipitation (prec), maximum (tmax), and minimum (tmin) temperature are combined to create a multidimensional data called tensor (a multidimensional array). In this paper, we propose a spatio temporal principal component analysis to initialize CP decomposition component. We take full advantage of the spatial and temporal structure of the data in the initialization step for cp component analysis. The performance of our method is tested via comparison with most popular initialization method. We also run a clustering analysis to further show the performance of our analysis.

1. Introduction

Many places have experienced changes in rainfall resulting in floods, droughts, or intense rain (see Reidmiller et al. (2017)) and heat waves. This has caused a lot of concerns around the world and increased the need for solutions such as developing more reliable predictive and diagnostic tools for weather and climate related events. Many natural phenomena such as meteorological or flow variables may be simulated by numerically solving modeling equations. Numerical Earth System Models (ESMs), whether global or regional, remain the principal instruments for simulating atmospheric and hydrological processes by solving the governing physical equations over discretized spatial domains. However, these models face two main challenges: heavy computation times that limit scenario exploration and near-real-time forecasting, which constrains scenario exploration and real-time applications, and the exponential growth of data dimensionality as spatial resolution increases. These constraints motivated the development of statistical and machine-learning methods that emulate the physics-based models. Two common tasks have emerged: **downscaling**, which aims to generate high-resolution fields from low-resolution inputs, and **forecasting**, which predicts future states at fixed resolution. Convolutional neural networks are effective for learning spatial features in downscaling applications (Goodfellow et al., 2016; Wang et al., 2021; Höhle et al., 2020; Annau et al., 2023), but their reliance on Cartesian grids complicates their use with the non-rectangular meshes native to most ESMs (Balaji et al., 2019), making regridding part of pre-processing (Annau et al., 2023). Regridding such data can introduce artifacts and blur

ORCID(s): 0000-0001-8509-2124 (F. Sanogo)

physically homogeneous regions, potentially obscuring large-scale climate events such as the 2003 European drought (Ciais et al., 2005). Graph neural networks (Lam et al., 2023; Chen et al., 2023) partially address this issue by operating on irregular grids for forecasting, yet they often demand extensive training resources and high-performance computing infrastructures.

Dimensionality-reduction methods offer an alternative pathway. Principal Component Analysis (PCA) (Jolliffe and Cadima, 2016; Bishop, 2006) also known in the climate sciences as Empirical Orthogonal Function analysis (Hannachi et al., 2007; Monahan et al., 2009)—is the standard tool for deriving compact spatial and temporal representations. While PCA efficiently extracts dominant variance patterns, it treats variables independently and imposes orthogonality constraints that lack clear physical interpretation (Hannachi et al., 2007).

Tensor decomposition techniques such as Canonical Polyadic decomposition (CPD) are designed to address these limitations. The Canonical Polyadic (CP) decomposition (Hong et al., 2020; Kruskal, 1977; Hitchcock, 1927; Carroll and Chang, 1970; Harshman, 1970), generalize PCA by modeling multi-dimensional relationships across space, time, and variables without enforcing orthogonality. CP expresses a tensor as a sum of rank-one components, enabling interpretable latent-factor discovery and providing a scalable framework for analyzing multiway climate datasets (Aggarwal, 2015; Lathauwer and De Moor, 1997). By decomposing a tensor into rank-one components, CP decomposition enables latent factor and hidden patterns or structures discovery in multiple-axes data analysis across many fields. It was introduced by Hitchcock (1927) as the polyadic decomposition and later by Carroll and Chang (1970) (CANDECOMP) and Harshman (1970) (PARAFAC); the unified term is CP Decomposition. Although tensor approaches are gaining traction in spatio-temporal data analysis (Hong et al., 2020; Xu et al., 2021; Tian et al., 2023), their application to climate research remains limited, especially regarding how spatial and temporal dependencies are incorporated into the initialization and estimation process. These factorizations yield low-dimensional, mode-specific factors (e.g., space, time, variable) and are often used as the basis for a clustering analysis to reveal coherent climate regimes. In fact, climate and meteorological studies often rely on categorizing data (observations or variables) into distinct subgroups with similar characteristics within groups (i.e. clustering). This is essential, as it allows for climate regionalization, it identify patterns such synoptic types Sheridan and Lee (2011). Clustering is a powerful tool that can help facilitate the analysis of meteorological events. In forecast analysis and evaluation, clustering can help in assessing the uncertainty and performance of forecasting models. It is often preceded by a dimensionality reduction technique like PCA due to the high dimensionality nature of climate data Gong and Richman (1995); Sheridan and Lee (2011).

In this work, we propose a spatio-temporal initialization strategy for CP decomposition that explicitly exploits the inherent structure of climate data. By initializing factor matrices using spatio-temporal principal components, our approach improves factor identifiability, and reconstruction accuracy, compared with standard methods such as random

or HOSVD-based initialization. Furthermore, we applied clustering to the resulting factor matrices, with performance assessed via silhouette scores. Our main contributions are:

- (1) A novel initialization procedure for CP decomposition that leverages spatio-temporal correlations to enhance reconstruction quality and interpretability.
- (2) An empirical evaluation on NCAR precipitation and temperature datasets, benchmarking against common initialization methods.
- (3) A clustering analysis illustrating the interpretive value of CP-derived factors and the performance of our model.

The remainder of the paper is organized as follows. Section 2 describes the studied dataset and its spatial–temporal structure. Section 3 details the proposed methodology. Section 4 presents experimental results and comparative analyses.

2. Data overview

For our analysis we considered a dataset, which includes three variables total precipitation (prec), maximum temperature (tmax) and minimum temperature (tmin) daily value over from January 1st, 1979 to December 31st, 2024. These variables are important for hydrological type studies. The variables were sourced from the NA-CORDEX data collection, available via the NCAR Climate Data Gateway website (<https://doi.org/10.5065/D6SJ1JCH>). They are output from the Canadian Regional Climate Model (CRCM5-OUR), which was run under the evaluation scenario forced by ERA-Interim reanalyses. To focus on information solely provided by the regional climate model we use the data with no interpolation or bias correction. The database covers North America with a regular grid (native rotated-pole grid) with 340 cells in longitude and 300 cells in latitude. The spatial resolution is 0.22° (50 km) (Mearns et al., 2017). For this paper, we restricted the domain to the New England - which includes six states: Maine, New Hampshire, Vermont, Massachusetts, Rhode Island, and Connecticut - region in the United States, 31 cells in longitude and 34 cells in latitude for a total of 1054 grid cells.

2.1. Notations

Let $1 \leq i \leq I$ a time index, $1 \leq j \leq J$ a location index and $1 \leq k \leq K$ an index that represents the physical variable of interest. Let $\mathbf{x}_{i,k} \in \mathbb{R}^J$ be a vector representing all the values of variable k at time step i over all the locations. Let $\mathbf{X}_k \in \mathbb{R}^{I \times J}$ be a matrix that combines $\mathbf{x}_{i,k}$ row-wise and contains all the values of variable k at all time steps and all locations. Lastly, let $\mathcal{X} \in \mathbb{R}^{I \times J \times K}$ be a mode 3 tensor that stacks \mathbf{X}_k for all the variables k .

In our case, we consider \mathbf{X}_1 , \mathbf{X}_2 and $\mathbf{X}_3 \in \mathbb{R}^{13149 \times 1054}$ be the matrices holding, respectively, the prec, tmax and tmin data described above. Moreover, let $\mathcal{X} \in \mathbb{R}^{13149 \times 1054 \times 3}$ be the mode 3 tensor stacking all three climate variables together.

2.2. Spatial properties

Here our analysis focus on the spatial properties of the climate variables for each of the four continental seasons: winter (from December to January), spring (from March to May), summer (from June to August) and fall (from September to November). To emphasize spatial patterns, we look at maps of Spearman correlation coefficients. Figure 1 shows Spearman correlation coefficients computed with respect to the reference location indicated by the black square (same color scale across all panels). In all panels, correlations decrease with distance from the reference location. The correlation coefficients are mostly positive. The patterns for tmax and tmin are broadly similar, with slight differences in winter and summer compared to precipitation's. tmax and tmin correlations remain strong in all seasons, with minor reductions in spatial extent during summer. Precipitation (left column) exhibits weaker and more spatially variable correlations compared to temperature.

2.3. Temporal properties

Next, we focus on the temporal properties of the climate variables by looking at the auto-correlation functions per season at a given grid box, see Fig. 2. Again we use Spearman correlation coefficients. The conclusions are similar to those drawn from the spatial patterns in Fig. 1. As seen in 2 the auto-correlation function of prec (first column) is very weak, much weaker than in the spatial case. The temporal dependence of tmax and tmin on the other hand shows clear variation with the season, with stronger dependence in spring and fall. Moreover, the shapes of the auto-correlation functions of tmax and tmin are very much alike.

3. Methodology

3.1. Spatio-Temporal Principal Component Analysis

Principal component analysis (PCA) is a powerful and widely used method in multivariate statistics. Principal Component Analysis (PCA) Hotelling (1933) can be performed on the sample covariance matrix $\mathbf{S} = \frac{1}{i} \mathbf{X}_k^T \mathbf{X}_k$, where \mathbf{X}_k is an $I \times J$ centered data matrix (observations of j variables on i independent objects). However, this approach do not take into account the dependence among nearby locations, when applied to spatial (geographic) data. The eigenvalues are nonnegative, and the principal components are given by the eigenvectors associated with the positive eigenvalues. Cliff addressed this by introducing the concept of 'spatial autocorrelation'. Incorporating this into PCA requires specifying a spatial-weights matrix \mathbf{W} that encodes neighborhood or proximity relations among the spatial units under study. Several literature on spatial PCA (SPCA) discusses how to define \mathbf{W} (Demšar et al., 2013;

Spatio-Temporal CPD

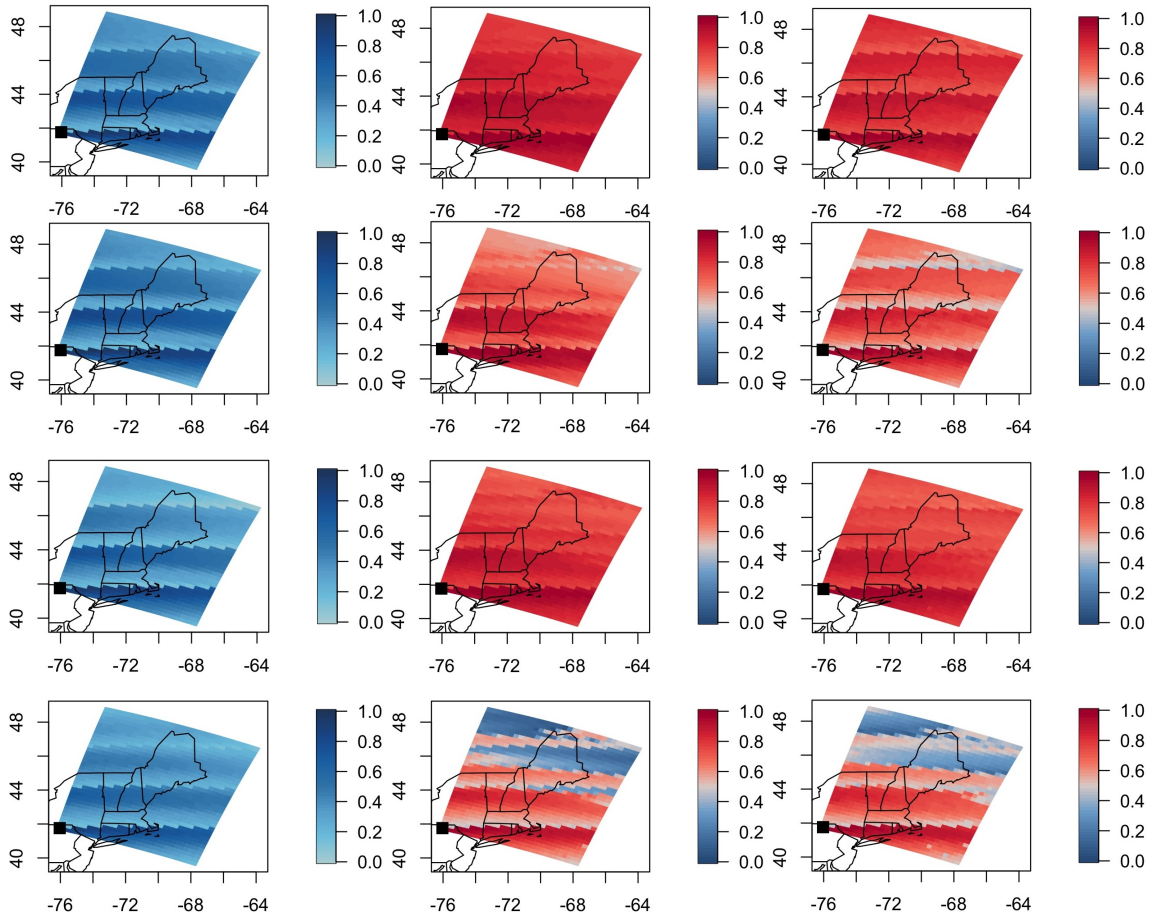


Figure 1: Spearman correlation coefficients in fall (Sept-Nov), winter (Dec-Jan), spring (Mar-May), summer (Jun-Aug) (in rows) with respect to the location indicated by the black square tile for prec, tmax and tmin (in columns).

Cartone and Postiglione, 2021; Virta et al., 2016). For this paper, our focus will be on Spatio Temporal Principal Component Analysis (STPCA); see Krzyśko et al. (2024). STPCA treats feature observations as functional time series, emphasizing their temporal evolution while preserving spatial structure. Its aim is to extract the dominant modes of variability in spatio-temporal data by jointly incorporating temporal dynamics, spatial relationships, and variation in feature magnitudes. To run an STPCA, analysis a list of matrices is considered with the rows representing i time steps and columns j locations or region of values of the k features/variables being considered. In fact, first the data matrix is transformed into a multivariate functional data set; see Górecki et al. (2018); Górecki and Krzyśko (2012). The transformation into a functional data is done by creating a matrix A of size $I \times pk$ through fourier basis eq. (1) and

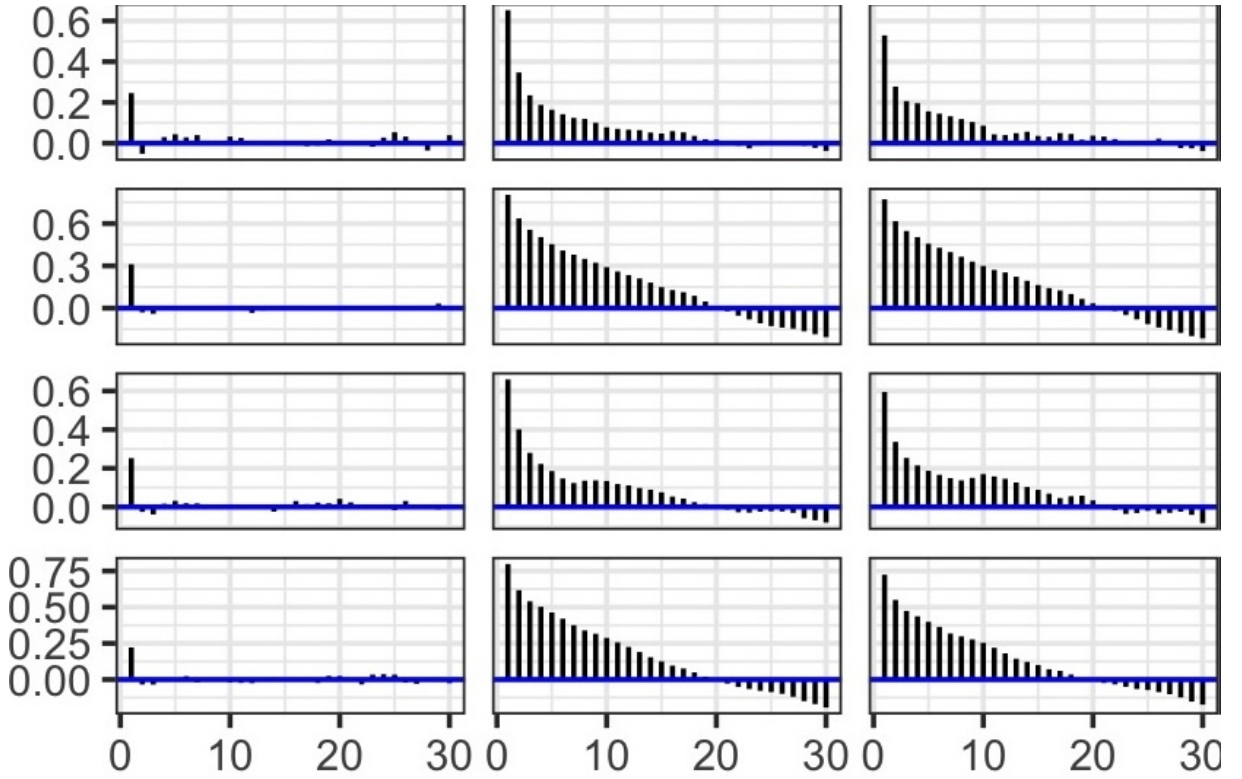


Figure 2: Winter (Dec-Jan), spring (Mar-May), summer (Jun-Aug) and fall (Sept-Nov) auto-correlation functions with lags expressed in days (in rows) for prec, tmax and tmin (in columns) at grid cell whose linear index is halfway through the flattened list of cells.

keeping the coefficients.

$$\begin{aligned}
 \phi_0(t) &= \frac{1}{\sqrt{T}}, & b &= 1, 2, \dots, \frac{B_k}{2}, \\
 \phi_{2b-1}(t) &= \sqrt{\frac{2}{T}} \sin\left(\frac{2\pi b t}{T}\right), & k &= 1, 2, \dots, m, \quad \text{with } B_k \text{ even.} \\
 \phi_{2b}(t) &= \sqrt{\frac{2}{T}} \cos\left(\frac{2\pi b t}{T}\right), & t &\in [0, n],
 \end{aligned} \tag{1}$$

The matrix A is then link to the spatial weight \mathbf{W} using the Moran's index (Moran, 1950) to obtain a spatial correlation matrix. This matrix is then used to find eigenvalues which, unlike standard PCA, can be either positive or negative. The associated set of eigenvectors denotes the spatiotemporal principal components, which are entirely dependent on the choice of \mathbf{W} . Changing the matrix \mathbf{W} changes the principal components, and thus the shape of the clusters of objects examined.

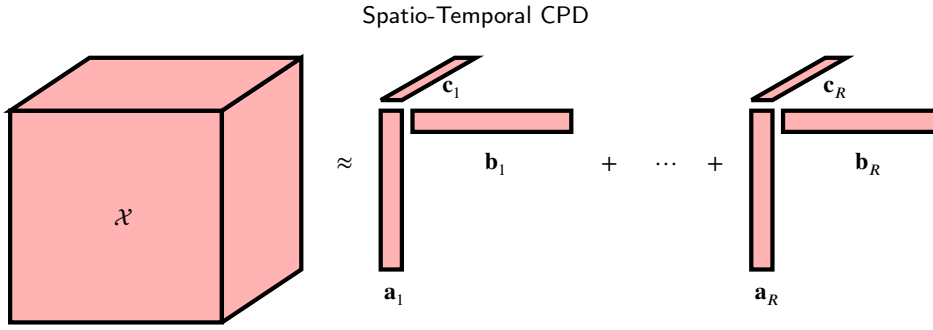


Figure 3: CP decomposition of a third order tensor $\mathcal{X} \in \mathbb{R}^{n \times p \times d}$ from (2).

3.2. CP decomposition

Let $\mathcal{X} \in \mathbb{R}^{I \times J \times K}$ be as above the mode 3 tensor that stacks along the third dimension The spatio-temporal variables and let R be the rank of \mathcal{X} . Then CPD would represent the tensor \mathcal{X} in the following form

$$\mathcal{X} = \sum_{r=1}^R \mathbf{a}_r \circ \mathbf{b}_r \circ \mathbf{c}_r = [[\mathbf{A}, \mathbf{B}, \mathbf{C}]], \quad (2)$$

where $\mathbf{A} = [\mathbf{a}_1 \dots \mathbf{a}_R] \in \mathbb{R}^{I \times R}$, $\mathbf{B} = [\mathbf{b}_1 \dots \mathbf{b}_R] \in \mathbb{R}^{J \times R}$ and $\mathbf{C} = [\mathbf{c}_1 \dots \mathbf{c}_R] \in \mathbb{R}^{K \times R}$ are called factor matrices. To determine the factor matrices of CPD in (2), the Alternating Least Square (ALS) approach is typically applied. ALS consists of finding each factor matrix in turn through gradient descent while fixing the other two (Liu et al., 2022). The CP decomposition from (2) is illustrated in Fig. 3.

While the Alternating Least Squares (ALS) algorithm is widely used for computing CP decomposition due to its simplicity and empirical success, its theoretical foundation, particularly regarding spatio-temporal data remain underdeveloped, especially in noisy, non-orthogonal, and higher-rank settings. It is also known that the loss surface can be highly non-convex with exponentially many local minima (Arous et al., 2018) when the signal to noise ratio is not sufficiently strong, making convergence to the true loading vectors theoretically uncertain with ALS. Initialization is then crucial for the success of ALS. For rank being 1 methods like Higher-Order Singular Value Decomposition (HOSVD) have proven to be an effective initializations; see Zhang and Xia (2018). This is the motivation for our method were the initialization regularize to all rank. In our method, first we find the Spatio-Temporal Principal Component, then find the factor matrices using the components, and finally using those factor as initial factor to find the CP factor via ALS. Recently, Tang et al. (2025) proposed a hybrid initialization strategy—Tucker-based Approximation with Simultaneous Diagonalization (TASD). The method uses Tucker decomposition to compress the tensor followed by SimDiag (Leurgans et al., 1993; Naskovska and Haardt, 2016) applied to the low-dimensional core establishing a statistical guarantees for general rank R . However, currently there are no initialization method that is built specifically to consider the spatial and temporal component of a spatio-temporal data. Our method reaches the same level of relative

error like T ASD even without the extra step of applying SimDiag which increase the time the initialization of the factor matrices for CP decomposition actually takes. The initialization step with STPCA is much faster compared to T ASD.

3.3. K means clustering

K-means is an unsupervised clustering algorithm, which divides unlabeled data into a certain number (commonly denoted as K) of distinct groupings by minimizing Euclidean distances between them Bauckhage (2015). It assumes that the closer the distance between two points, the greater the similarity. k-means is primarily designed for low-array datasets, making it unsuitable for handling high-dimensional tensor datasets. Applying tensor decomposition model into K-means clustering algorithm can accurately find the multilinear subspaces of data and cluster these high-order data at the same time. In our analysis the goal is to find the subspace of our high-dimensional data using CPD and use k-means clustering to cluster the latent factor along the tensor mode into k groups. K-means can be generalized to tensor spaces using a tensor decomposition. Considering our third order tensor $\mathbb{R}^{n \times p \times d}$ with CPD factor $\mathbf{A} \in \mathbb{R}^{I \times R}$, $\mathbf{B} \in \mathbb{R}^{J \times R}$, $\mathbf{C} \in \mathbb{R}^{K \times R}$, and R is the CP rank. Clustering is applied to the rows of A .

$$\min_{\mathbf{A}, \mathbf{B}, \mathbf{C}, \mathbf{S}, \mathbf{D}} \|\mathbf{X}_1 - \mathbf{DA}(\mathbf{C} \odot \mathbf{B})^T\|_F^2 + \lambda \|\mathbf{A} - \mathbf{SC}\|_F^2 + \eta(\|\mathbf{B}\|_F^2 + \|\mathbf{C}\|_F^2). \quad (3)$$

The second term represents the *K-means penalty*, while the last term regularizes the factors. This optimization problem is done under the following constraints:

$$\mathbf{A}, \mathbf{B}, \mathbf{C} \geq 0, \quad \|\mathbf{S}(n, :)\|_0 = 1. \quad (4)$$

The algorithm iterates updates for clustering, decomposition, and factor matrices until convergence.

Performance Measure. To evaluate how well the clusters from kmeans are separated for CP Decomposition, we use the silhouette score. The Silhouette coefficient is based on the dissimilarity of a component to all other components within the same cluster (intra-cluster distance) and the distance of the component to the nearest cluster (inter-cluster distance). The intra-cluster distances and the nearest-cluster distances are averaged for each component (denoted as ‘a’ and ‘b’, respectively), and the Silhouette Coefficient is computed by $\frac{b-a}{\max(a,b)}$ (Rousseeuw, 1987). This assess how well-separated and compact the clusters are.

4. Results and discussion

In this section we have two types of numerical experiments for testing the performance of our algorithm. The first one is applying our dataset describe in section 2 to run a CPD decomposition and compare performance using the

Spatio-Temporal CPD

Initialization	Relative error for rank = 2	Relative error for rank = 3
HOSVD	0.4928	0.3832
Random	0.4930	0.3849
STPCA	0.4910	0.3810

Table 1

Relative reconstruction errors for CPD with ALS where $\mathcal{X} \in \mathbb{R}^{13149 \times 1054 \times 3}$.

Initialization	Silhouette Scores for mode 1	Best k	Silhouette Scores for mode 2	Best k
HOSVD	0.6484	2	0.5872	2
Random	0.658	2	0.6	2
STPCA	0.7990	2	0.6184	4

Table 2

Silhouette scores for k-means clustering applied to CPD components with rank 2

relative error given by $\frac{\|\mathcal{X}_{\text{estimate}} - \mathcal{X}\|_2}{\|\mathcal{X}\|_2}$. The second experiment is a Kmeans clustering analysis done to again test the performance of our method compared to existing ones.

4.1. STPCA-CPD using Alternating Least Square method

In the following experiments we applied the STPCA-CPD algorithm to the real dataset describe in section 2. We did the decomposition varying the number of components (i.e. the rank). We also compare the performance of our algorithm with the well known HOSVD+CPD where the initialization of the factor matrices is done using Higher Order Singular Value Decomposition (HOSVD), and a random initialization coupled with using ALS to find the CP factor matrices. We compute the reconstruction error using the relative error for each method. All the decompositions for HOSVD+CPD and random+CPD were computed using the matlab tensor toolbox (Kolda and Bader, 2009; Bader et al., 2024).

The overall the CPD with STPCA as initializer perform better with a relative error lower than the other methods see Table 1. Note that for this analysis we only used 2 and 3 components but still ended up with a good results. The method is applicable to n number of components.

4.2. Clustering analysis of the CP factors per mode

To continue this analysis we are now looking at the K-means clustering (see section 3.3) of the CPD factors with the initialization methods used above. The goal in this case is to use the components from all the method in mode 1 (temporal mode) and mode 2 (spatial mode), and do a K-means clustering analysis. We use the silhouette score as described in section 3.3. The k-means analysis run through a range of k from 2 to 12 for all the decompositions. Table 2 shows the results for rank 2 and Table 3 shows the results for rank 3. In both cases, STPCA+CPD outperform the other methods.

Spatio-Temporal CPD

Initialization	Silhouette Scores for R =2	Best k	Silhouette Scores for R = 3	Best k
HOSVD	0.4932	3	0.6528	2
Random	0.513	3	0.648	2
STPCA	0.6456	2	0.6721	2

Table 3

Silhouette scores for k-means clustering applied to CPD components with rank 3

5. Conclusions

In this study, we employed a Spatio-Temporal Principal Component Analysis (STPCA) to initialize the factors in our CANDECOMP/PARAFAC (CP) decomposition, which was subsequently optimized using the Alternating Least Squares (ALS) algorithm. The numerical experiments yielded promising results, demonstrating a distinct advantage in leveraging the spatio-temporal dependencies inherent in the data into the CP factorization process. Model performance was assessed through the computation of the relative reconstruction error for each configuration.

Furthermore, we applied k-means clustering to the extracted factor matrices and evaluated clustering quality using silhouette scores. The proposed STPCA+CPD approach consistently outperformed baseline methods, confirming the benefits of our initialization strategy.

For future research, this framework could be extended by integrating deep learning architectures to enhance its capacity to capture complex spatio-temporal dynamics. Additionally, we plan to investigate more robust spatio-temporal tensor decomposition schemes and to generalize the tensor framework for forecasting and downscaling applications.

6. Acknowledgments

The author would like to thank Professor Julie Carreau for helpful discussion concerning this project.

Code availability section

All data is publicly available and cited. Code available upon request.

References

- Aggarwal, C.C., 2015. Data Mining: The Textbook. Springer. URL: <https://link.springer.com/book/10.1007/978-3-319-14142-8>.
- Annau, N., Cannon, A., Monahan, A., 2023. Algorithmic hallucinations of near-surface winds: Statistical downscaling with generative adversarial networks to convection-permitting scales. Artificial Intelligence for the Earth Systems 2, e230015. URL: <https://journals.ametsoc.org/view/journals/aies/2/4/AIES-D-23-0015.1.xml>, doi:10.1175/AIES-D-23-0015.1.
- Arous, G.B., Mei, S., Montanari, A., Nica, M., 2018. The landscape of the spiked tensor model. URL: <https://arxiv.org/abs/1711.05424>, arXiv:1711.05424.
- Bader, B.W., Kolda, T.G., et al., 2024. MATLAB Tensor Toolbox, Version 3.6. <https://www.tensortoolbox.org/>. Available from Sandia National Laboratories.

- Balaji, V., Adcroft, A., Liang, Z., 2019. Gridspec: A standard for the description of grids used in earth system models. URL: <https://arxiv.org/abs/1911.08638>, arXiv:1911.08638.
- Bauchhage, C., 2015. K-means clustering is matrix factorization. arXiv preprint arXiv:1512.07548 .
- Bishop, C., 2006. Pattern Recognition and Machine Learning. Springer. URL: <https://www.microsoft.com/en-us/research/publication/pattern-recognition-machine-learning/>.
- Carroll, J.D., Chang, J., 1970. Analysis of individual differences in multidimensional scaling via an n-way generalization of "eckart-young" decomposition. *Psychometrika* 35, 283–319.
- Cartone, A., Postiglione, P., 2021. Principal component analysis for geographical data: the role of spatial effects in the definition of composite indicators. *Spatial Economic Analysis* 16, 126–147. URL: <https://doi.org/10.1080/17421772.2020.1775876>, doi:10.1080/17421772.2020.1775876, arXiv:<https://doi.org/10.1080/17421772.2020.1775876>.
- Chen, K., Han, T., Gong, J., et al., 2023. Fengwu: Pushing the skillful global medium-range weather forecast beyond 10 days lead. arXiv preprint arXiv:2304.02948 .
- Ciais, P., Reichstein, M., Viovy, N., Granier, A., Ogee, J., Allard, V., Aubinet, M., Buchmann, N., Bernhofer, C., Carrara, A., Chevallier, F., Noblet, N.D., Friend, A.D., Friedlingstein, P., Grünwald, T., Heinesch, B., Keronen, P., Knohl, A., Krinner, G., Loustau, D., Manca, G., Matteucci, G., Miglietta, F., Ourcival, J.M., Papale, D., Pilegaard, K., Rambal, S., Seufert, G., Soussana, J.F., Sanz, M.J., Schulze, E.D., Vesala, T., Valentini, R., 2005. Europe-wide reduction in primary productivity caused by the heat and drought in 2003. *Nature* 437, 529–533.
- Cliff, A., . Ord., jk, 1969. the problem of spatial autocorrelation. London papers in regional science (1), studies in regional science. London: Pion , 25–55.
- Demšar, U., Harris, P., Brunson, C., Fotheringham, A.S., McLoone, S., 2013. Principal component analysis on spatial data: An overview. *Annals of the Association of American Geographers* 103, 106–128. URL: <https://doi.org/10.1080/00045608.2012.689236>, doi:10.1080/00045608.2012.689236, arXiv:<https://doi.org/10.1080/00045608.2012.689236>.
- Gong, X., Richman, M., 1995. On the application of cluster analysis to growing season precipitation data in north america east of the rockies. *Journal of Climate* 8, 897–931. doi:10.1175/1520-0442(1995)008<0897:OTA0CA>2.0.CO;2.
- Goodfellow, I., Bengio, Y., Courville, A., 2016. Deep learning. MIT press.
- Górecki, T., Krzyśko, M., 2012. Functional principal components analysis. *Data analysis methods and its applications* , 71–87.
- Górecki, T., Krzyśko, M., Waszak, Ł., Wołyński, W., 2018. Selected statistical methods of data analysis for multivariate functional data. *Statistical Papers* 59, 153–182.
- Hannachi, A., Jolliffe, I.T., Stephenson, D.B., 2007. Empirical orthogonal functions and related techniques in atmospheric science: A review. *International Journal of Climatology* 27, 1119–1152. URL: <https://rmets.onlinelibrary.wiley.com/doi/abs/10.1002/joc.1499>, doi:<https://doi.org/10.1002/joc.1499>, arXiv:<https://rmets.onlinelibrary.wiley.com/doi/pdf/10.1002/joc.1499>.
- Harshman, R., 1970. Foundations of the parafac procedure: Models and conditions for an " explanatory" multimodal factor analysis. *UCLA Working Papers in Phonetics* 16, 84.
- Hitchcock, F.L., 1927. The expression of a tensor or a polyadic as a sum of products. *Journal of Mathematics and Physics* 6, 164–189. URL: <https://onlinelibrary.wiley.com/doi/abs/10.1002/sapm192761164>, doi:<https://doi.org/10.1002/sapm192761164>, arXiv:<https://onlinelibrary.wiley.com/doi/pdf/10.1002/sapm192761164>.
- Hong, D., Kolda, T.G., Duersch, J.A., 2020. Generalized canonical polyadic tensor decomposition. *SIAM Review* 62, 133–163. URL: <https://doi.org/10.1137/18M1203626>, doi:10.1137/18M1203626, arXiv:<https://doi.org/10.1137/18M1203626>.
- Hottelling, H., 1933. Analysis of a complex of statistical variables into principal components. *Journal of educational psychology* 24, 417.

- Höhlein, K., Kern, M., Hewson, T., Westermann, R., 2020. A comparative study of convolutional neural network models for wind field downscaling. *Meteorological Applications* 27, e1961. URL: <https://rmets.onlinelibrary.wiley.com/doi/abs/10.1002/met.1961>, doi:<https://doi.org/10.1002/met.1961>, arXiv:<https://rmets.onlinelibrary.wiley.com/doi/pdf/10.1002/met.1961>.
- Jolliffe, I.T., Cadima, J., 2016. Principal component analysis: a review and recent developments. *Philosophical transactions of the royal society A: Mathematical, Physical and Engineering Sciences* 374, 20150202.
- Kolda, T.G., Bader, B.W., 2009. Tensor decompositions and applications. *SIAM Review* 51, 455–500. URL: <https://doi.org/10.1137/07070111X>, doi:10.1137/07070111X, arXiv:<https://doi.org/10.1137/07070111X>.
- Kruskal, J.B., 1977. Three-way arrays: rank and uniqueness of trilinear decompositions, with application to arithmetic complexity and statistics. *Linear Algebra and its Applications* 18, 95–138. URL: <https://www.sciencedirect.com/science/article/pii/0024379577900696>, doi:[https://doi.org/10.1016/0024-3795\(77\)90069-6](https://doi.org/10.1016/0024-3795(77)90069-6).
- Krzyżko, M., Nijkamp, P., Ratajczak, W., Wołyński, W., Wenerska, B., 2024. Spatio-temporal principal component analysis. *Spatial Economic Analysis* 19, 8–29. URL: <https://doi.org/10.1080/17421772.2023.2237532>, doi:10.1080/17421772.2023.2237532, arXiv:<https://doi.org/10.1080/17421772.2023.2237532>.
- Lam, R., Sanchez-Gonzalez, A., Willson, M., et al., 2023. Learning skillful medium-range global weather forecasting. *Science* 382, 1416–1421. URL: <https://www.science.org/doi/abs/10.1126/science.adi2336>, doi:10.1126/science.adi2336, arXiv:<https://www.science.org/doi/pdf/10.1126/science.adi2336>.
- Lathauwer, L., De Moor, B., 1997. From matrix to tensor: Multilinear algebra and signal processing. *Mathematics in Signal Processing IV*, 1–15.
- Leurgans, S.E., Ross, R.T., Abel, R.B., 1993. A decomposition for three-way arrays. *SIAM Journal on Matrix Analysis and Applications* 14, 1064–1083. URL: <https://doi.org/10.1137/0614071>, doi:10.1137/0614071, arXiv:<https://doi.org/10.1137/0614071>.
- Liu, Y., Liu, J., Long, Z., Zhu, C., 2022. *Tensor computation for data analysis*. Springer.
- Mearns, L., McGinnis, S., Korytina, D., et al., 2017. The na-cordex dataset, version 1.0. NCAR Climate Data Gateway Boulder CO, accessed 08/11/2021 doi:<https://doi.org/10.5065/D6SJ1JCH>.
- Monahan, A.H., Fyfe, J.C., Ambaum, M.H.P., Stephenson, D.B., North, G.R., 2009. Empirical orthogonal functions: The medium is the message. *Journal of Climate* 22, 6501 – 6514. URL: <https://journals.ametsoc.org/view/journals/clim/22/24/2009jcli3062.1.xml>, doi:10.1175/2009JCLI3062.1.
- Moran, P.A., 1950. A test for the serial independence of residuals. *Biometrika* 37, 178–181.
- Naskovska, K., Haardt, M., 2016. Extension of the semi-algebraic framework for approximate cp decompositions via simultaneous matrix diagonalization to the efficient calculation of coupled cp decompositions, in: 2016 50th Asilomar Conference on Signals, Systems and Computers, pp. 1728–1732. doi:10.1109/ACSSC.2016.7869678.
- Reidmiller, D., Avery, C., Easterling, D., Kunkel, K., Lewis, K., Maycock, T., Stewart, B., Program, U.G.C.R., Oceanic, N., Administration, A., Aeronautics, N., Administration, S., 2017. Impacts, risks, and adaptation in the united states: Fourth national climate assessment, volume ii. URL: <https://doi.org/10.7930/NCA4.2018>.
- Rousseeuw, P.J., 1987. Silhouettes: A graphical aid to the interpretation and validation of cluster analysis. *Journal of Computational and Applied Mathematics* 20, 53–65. URL: <https://www.sciencedirect.com/science/article/pii/0377042787901257>, doi:[https://doi.org/10.1016/0377-0427\(87\)90125-7](https://doi.org/10.1016/0377-0427(87)90125-7).
- Sheridan, S., Lee, C., 2011. The self-organizing map in synoptic climatological research. *Progress in Physical Geography* 35, 109–119. doi:10.1177/0309133310397582.

- Tang, R., Chhor, J., Klopp, O., Zhang, A.R., 2025. Revisit cp tensor decomposition: Statistical optimality and fast convergence. URL: <https://arxiv.org/abs/2505.23046>, arXiv:2505.23046.
- Tian, F., Kilmer, M.E., Miller, E., Patra, A., 2023. Tensor bm-decomposition for compression and analysis of spatio-temporal third-order data. arXiv:2306.09201.
- Virta, J., Taskinen, S., Nordhausen, K., 2016. Applying fully tensorial ica to fmri data, in: 2016 IEEE Signal Processing in Medicine and Biology Symposium (SPMB), pp. 1–6. doi:10.1109/SPMB.2016.7846858.
- Wang, F., Tian, D., Lowe, L., Kalin, L., Lehrter, J., 2021. Deep learning for daily precipitation and temperature downscaling. Water Resources Research 57, e2020WR029308. URL: <https://agupubs.onlinelibrary.wiley.com/doi/abs/10.1029/2020WR029308>, doi:<https://doi.org/10.1029/2020WR029308>, arXiv:<https://agupubs.onlinelibrary.wiley.com/doi/pdf/10.1029/2020WR029308>. e2020WR029308 2020WR029308.
- Xu, J., Zhou, J., Tan, P., Liu, X., Luo, L., 2021. Spatio-temporal multi-task learning via tensor decomposition. IEEE Transactions on Knowledge and Data Engineering 33, 2764–2775. doi:10.1109/TKDE.2019.2956713.
- Zhang, A., Xia, D., 2018. Tensor svd: Statistical and computational limits. IEEE Transactions on Information Theory 64, 7311–7338. doi:10.1109/TIT.2018.2841377.